American Journal of Pathology, Vol. 150, No. 6, June 1997

Adult *Schistosoma mansoni* Worms Positively Modulate Soluble Egg Antigen-Induced Inflammatory Hepatic Granuloma Formation *in Vivo*

Stereological Analysis and Immunophenotyping of Extracellular Matrix Proteins, Adhesion Molecules, and Chemokines

Werner Jacobs,* Johannes Bogers,* Andre Deelder,† Marc Wéry,‡ and Eric Van Marck*

From the Laboratory of Pathology, Universitaire Instelling Antwerpen, and the Laboratory of Protozoology,‡ Prince Leopold Institute for Tropical Medicine, Antwerpen, Belgium, and the Laboratory of Parasitology,† Rijksuniversiteit Leiden, Leiden, The Netherlands*

Synchronized liver granulomas were induced by injecting Sepharose beads to which SEA soluble egg antigen (SEA) or the concanavalin A binding fraction of SEA had been coupled into a mesenteric vein in naive, single-sex (35 days) and bisexually (28 days)* Schistosoma mansoni*-infected and* Plasmodium berghei*-immunized mice. Stereological analysis revealed that peak granuloma formation was already reached 8 days after injection in single-sex infected mice compared with 16 days in naive animals. No difference in granuloma formation between naive and* P. berghei*-immunized animals and between unisexually and bisexually* S. mansoni*-infected mice was observed. This suggests that the positive immunomodulatory effect on the granulomogenesis is worm specific and not likely to be due to arousal of the immune system by unrelated factors, nor is it influenced by the gender or degree of maturation of female worms. At all stages in time, the concanavalin A binding-fraction-induced granulomas reached only 65 to 70% of the volume of SEA-induced granulomas. Immunophenotyping of extracellular matrix proteins around deposited beads revealed that fibronectin was the dominant extracellular matrix protein and that also type I and IV collagen and laminin were deposited. Temporal analysis of the expression of the adhesion molecules ICAM-1, LFA-1, VLA-4, and VLA-6 was performed. Morphological evidence is presented for the role of adhesion molecules in the initiation and maintenance of hepatic granuloma formation. The chemokine monocyte chemoattractant protein-1 was expressed in the granuloma and in hepatic artery branches. From these data, it is concluded that adult* S. mansoni *worms positively modulate schistosomal hepatic granuloma formation* in vivo. *Adhesion molecules and chemokines play important roles in schistosomal granuloma formation. (Am J Pathol 1997, 150:2033–2045)

Schistosomiasis mansoni is a parasitic disease caused by the blood fluke *Schistosoma mansoni*. Schistosomes are antigenically very complex organisms, and stage-specific antigens are found among schistosomula, cercariae, eggs, or adult worms.[1,2] The pathology of the disease is induced by the host's

Supported by the grants 9.0302.95 and 1.5.043.96N of the Belgian National Fund for Scientific Research (NFWO). W. Jacobs is a research assistant of the NFWO.

Accepted for publication March 13, 1997.

Address reprint requests to Dr. E. Van Marck, Universitaire Instelling Antwerpen (U.I.A.), Laboratory of Pathology, Universiteitsplein 1, B-2610 Antwerpen (Wilrijk), Belgium.

granulomatous response to deposited eggs, primarily in the liver and intestines.[3] The granulomatous hypersensitivity reaction around deposited eggs is mediated by T-cell responses to the secreted soluble egg antigens (SEAs).[3–5] In the past, great effort has been made to determine the egg antigen(s) that elicited T-cell responses and induced granuloma formation.[6–10] It was found that some of these egg antigens are both granulomogenic and cross-reactive with schistosomular antigens.[11] However, there is only little information available concerning the *S. mansoni* adult worm antigen fractions that mediate granuloma reactivity. SEAs and soluble worm antigens (SWAPs) exert differential cytokine responses in both human and experimental murine infection. It was demonstrated that leukocytes responded with a Th2 pattern of cytokine production to egg antigens but with a Th0 pattern to worm antigens in both human schistosomiasis patients[12] and in experimental murine schistosomiasis.[13] In human schistosomiasis, these cytokine responses are, however, strongly dependent on the clinical form as interferon-γ production by peripheral blood mononuclear cells stimulated with SWAP is only observed in patients with acute or hepatosplenic schistosomiasis and is absent in the intestinal form.[12,14] An accelerated reaction against injected SEA-coupled beads in the liver was empirically seen in animals sensitized with schistosome worms.[15] Glycoproteins derived from adult male worms were shown to induce a modest granulomatous reaction.[9] Very recently, Hirsch et al[16] reported that fractionated *S. mansoni* adult worm antigens coupled to polyacrylamide beads were able to induce granuloma formation *in vitro*. These data indicate that the immunological processes responsible for granuloma formation may not be absolutely egg-stage specific.

Intercellular adhesion molecule-1 (ICAM-1) expression can be induced by products of deposited *S. mansoni* eggs.[17] Attention has therefore been focused on the role of adhesion molecules in *S. mansoni*-induced granulomogenesis. Lukacs et al[18] demonstrated that inflammatory granuloma formation was mediated by tumor-necrosis-factor-α-inducible ICAM-1. Blockade of the adhesion molecules ICAM-1, lymphocyte function-associated antigen-1 (LFA-1), and very late antigen-4 (VLA-4) by monoclonal antibodies inhibited spleen and granuloma interleukin-2 and -4 production in schistosomiasis mansoni.[19] Furthermore, lymphocytes can interact with extracellular matrix (ECM) proteins through the VLA adhesion molecules present on their cell membrane. Interactions between VLA-4 and -5/fibronectin and VLA-6/laminin have been well characterized.[20] In addition, recent studies have demonstrated that there is a significant interplay between chemokines and adhesion molecules. Macrophage inflammatory protein (MIP)-1β induced binding of T cells to vascular cell adhesion molecule-1 (VCAM-1) *in vitro*.[21] Recently, the role of the chemokines monocyte chemoattractant protein-1 (MCP-1)[22] during the secondary inflammatory response and MIP-1α[23] during the primary response against *S. mansoni* eggs was elucidated.

The present study was undertaken to analyze the *in vivo* granulomatous response in naive and single-sex *S. mansoni*-infected mice toward beads coupled with crude SEA or a concanavalin A (ConA) binding fraction that were implanted into the liver. *Plasmodium berghei*-immunized and bisexually *S. mansoni*-infected animals served, respectively, to evaluate the effect of aspecific immune modulation and worm gender on the granulomogenesis. The nature of the ECM proteins deposited around the antigen-coupled beads and the temporal expression pattern of the adhesion molecules ICAM-1, LFA-1, VLA-4, and VLA-6 and the chemokine MCP-1 was assessed.

Materials and Methods

Animals

Six-week-old, male OF1 mice and Syrian golden hamsters were purchased from Iffa Credo (St.-Germain sur L'Arbresle, France). All animals received water and food *ad libitum*. The animals received humane care according to the institution's guidelines. All experiments were conducted under the supervision of an animal welfare officer.

Preparation of Antigens and Antigen-Coupled Beads

The preparation of antigen-coupled beads is described in full by Deelder et al.[24] Briefly, SEA was prepared from isolated *S. mansoni* eggs from infected hamsters (48 days after infection) according to the technique described by Browne and Thomas.[25] After homogenization and centrifugation (25,000 $\times$ *g* for 45 minutes) of the eggs, the SEA-containing supernatant was dialyzed against distilled water (4°C) overnight. For the isolation of glycoprotein antigens from SEA, the technique described by Pelley et al[26] was used. SEA was applied to a column of 15 $\times$ 1.6 cm filled with ConA-Sepharose 4B (Pharmacia, Uppsala, Sweden) and eluted (flow rate, 30 ml/hour). Two nonbinding frac-

tions designed ConA A and B were eluted from the column. In an earlier study, these two fractions were shown not to be granulomogenic.[15] A third fraction (ConA binding fraction) was eluted from the column with 0.2 mol/L α-2-methyl-D-mannoside. This fraction was dialyzed 24 hours against distilled water and freeze-dried. Sepharose CL4B beads (Pharmacia) were wet-sieved to obtain a fraction with a diameter between 63 and 75 μm. Beads were activated with 50 mg of CNBr/ml beads and antigen, SEA, or ConA binding fraction were coupled at a concentration of 2 and 1 mg of antigen/ml beads, respectively. After antigen coupling, beads were deactivated overnight with 4-aminobutyric acid and washed extensively with sterile phosphate-buffered saline (PBS) before injection. Unloaded beads (activated/deactivated) were used as a negative control. Homogeneous binding of the antigen to the beads was checked with immunofluorescence.

Experimental S. mansoni *Infections*

Unisexual Infections

Unisexual *S. mansoni* infections were obtained through infection of mice with cercariae shed by *Biomphalaria glabrata* snails infected with a single miracidium. This was achieved as follows. A hamster infected with 1400 cercariae was sacrificed after 48 days and perfused through the heart with citrated PBS for 10 minutes. The liver was removed and mashed through a sieve with distilled water at 28°C. The suspension was left for 15 minutes and then put in front of a beam lamp. After 30 minutes, the miracidia were collected. An appropriate dilution of miracidia was made so that 10 μl of solution contained 1 miracidium most of the time. Ten microliters of the miracidia-containing suspension was then put on a glass slide and examined under a stereomicroscope. If only one miracidium were seen, the slide was dipped in a six-well plate containing one snail in aquarium water. The snails were kept in contact with the miracidia for 24 hours and were then placed in a dark room for 35 days. After 35 days, the snails were shed weekly. If cercariae were present, mice were infected with 100 cercariae (from one snail) per mouse.

Bisexual Infections

Mice were infected with 30 cercariae of a Puerto Rican strain of *S. mansoni* by a transcutaneous route. Bisexually infected mice served to evaluate a potential influence of worm gender or degree of maturation of the female worms on the immune response toward SEA-coupled beads. Bisexually infected mice were injected with SEA-coupled beads (28 days after infection) and sacrificed after 8 days. As eggs are deposited 4 to 6 weeks after cercarial penetration,[27] primary SEA sensitization had not occurred at the time of sacrifice.

Plasmodium berghei *Immunization*

Mice were immunised against *P. berghei* pre-erythrocytic (hepatic) stages to check whether an effect of unisexual infection on granuloma formation was specifically worm associated rather than due to an altered immune responsiveness. The immunization was carried out through tail vein injection three times at biweekly intervals with 50,000 viable sporozoites each time. After every sporozoite inoculation, the animals were given by oral gavage three doses of 60 mg/kg chloroquine base at days 1, 2, and 3 after injection to prevent blood infection. Blood was checked for parasites at day 8 after each injection to confirm the absence of parasite development. The success of the immunization was controlled using the immunofluorescent antibody technique.

Briefly, the glands of infected *Anopheles stephensi* mosquitoes were dissected and crushed in glucose lactalbumin serum hemoglobin with 10% fetal calf serum. The sporozoite suspension was centrifuged (13,000 rpm for 5 minutes), the supernatant discarded, and the pellet mixed with 1% glutaraldehyde in PBS. The mixture was centrifuged for 3 minutes and afterwards washed extensively with PBS azide. Drops of the parasite suspension were distributed on siliconized slides and air dried. The slides were brought in contact with the serum of immunized mice (dilutions 1/20 to 1/640 in PBS) for 30 minutes at 37°C. After extensive washing with PBS azide, the secondary antibody (fluorescein isothiocyanate (FITC)-conjugated goat anti-mouse IgG (dilution 1/100); Pasteur Diagnostics, Marnes-La-Coquille, France) in Evans blue (1/10,000) was applied for 30 minutes at 37°C. The slides were mounted with glycerine and examined with a fluorescence microscope. The fluorescent signal was quantified ranging from a fine green layer outlining the sporozoites (+) to strong fluorescence (+++).

Induction of Synchronous Granulomas

Synchronous granulomas were induced in mice that were infected by single-sex cercariae for 35 days or in bisexually infected mice 28 days after infection by injecting antigen-coupled beads in the cecal vein of

the mouse. The mouse was anesthetized (60 mg/kg pentobarbital intraperitoneally), and a midabdominal incision (2 cm) was made. The cecum was brought outside the body, and the cecal vein was visualized. At approximately 2 cm from the cecum tip, a major side branch was noticed in 80% of the animals. Two loops (Perma-hand Seide 7.0, Ethicon, Norderstedt, Germany) with a loose knot were applied around the vein, distal from the side branch. Twenty thousand beads dissolved in 0.3 ml of sterile PBS buffer were injected over a period of 10 seconds in the vein using an insulin syringe with a 29-gauge needle (Becton Dickinson, Dublin, Ireland). The distal loop was closed with the needle still in place. The proximal loop was then closed while gently removing the needle. The cecum was placed back inside the body and the incision was closed with ethilon 3.0 (Ethicon). Spitalen powder was applied to prevent wound infection. Unloaded beads were injected as negative controls. Sham-operated animals were exposed to the same procedure with injection of 0.3 ml of sterile PBS instead of antigen-coupled beads.

Stereological Analysis

Quantitative analysis of granuloma volume has almost exclusively been carried out by averaging the largest and perpendicular diameter of a granuloma and calculating the volume assuming the granuloma to be spherical and sectioned in a median plane. These two conditions are, however, bold assumptions, and the need for a (simple) method measuring the volume independent of the object's shape arises. Stereological techniques yielding quantitative information about geometric features of structures can be obtained from a test system of lower dimension than the *in vivo* structure itself.[28] In this study, we used one-dimensional (points) and two-dimensional (lines) test probes to obtain an estimation of a three-dimensional property (granuloma) from a two-dimensional object (histological slide). Volume estimation by point sampling provides a direct, more correct, and unbiased estimate of the mean volume from the volume distribution without any further assumption about the object shape than that of convexity.[29] Volume-weighted mean granuloma volume (MGV) was estimated using point-sampled intercepts. By point sampling, the granulomas are sampled directly proportional to their volume. Multiplication of the averaged, cubed mean intercept length with a constant gives an estimate of the MGV. Sirius-H-stained sections were examined using a Leitz 10× lens (numeric aperture 0.25) on a Leitz Orthoplan microscope (Leitz, Wetzlar, Germany), and the images were recorded using a Pulnix TM-765 monochrome camera (Pulnix Video Division, Basingstoke, UK). The image was viewed on a computer screen simultaneous with a randomly placed 12 × 12 grid generated by the computer software. The points hitting a granuloma were selected by the operator, after which the computer drew a randomly oriented line through the selected point. The operator marked the intercepts of this line with the boundaries of the granuloma, resulting in a point-sampled intercept. This procedure was repeated an average of 30 times. In general, a stable value for the MGV was obtained after 25 measurements. The volume-weighted MGV was calculated from the formula $MGV = \pi/3 \langle l \rangle^3$, where $\langle l \rangle$ is the mean length of the collected intercepts. A simple, cheap, and direct image analysis system specifically designed for stereological measurements was used (Stereology 2.0, Kinetic Imaging, Liverpool, UK), facilitating these measurements (analysis time was 15 minutes per liver).

Immunohistochemistry

The antibodies used in this experiment and their dilutions are listed in Table 1. We used three standard immunohistochemical procedures for this study. For all techniques, cold acetone-fixed (−20°C), 5-μm-thick cryostat sections were incubated overnight at 4°C with the primary antibody. Immunofluorescence was used for the antibodies directed against collagen I, collagen IV, fibronectin, laminin, and MCP (secondary antibody was FITC-conjugated goat anti-rabbit IgG). The alkaline phosphatase anti-alkaline phosphatase (APAAP) technique was applied for the antibodies directed against ICAM-1, LFA-1, and macrophages (secondary and tertiary antibodies, rabbit anti-rat IgG and rat APAAP complex (Dako, Glostrup, Denmark)). VLA-4 and VLA-6 were demonstrated using an indirect immunoperoxidase staining technique (secondary antibody was peroxidase-conjugated goat anti-rat IgG). The reaction product for the APAAP procedure was developed by incubation with the alkaline phosphatase substrate kit SK-5100 (Vector Laboratories, Burlingame, CA). Fluorescent detection of the alkaline phosphatase reaction product[30] could be carried out using a 543-nm excitation wavelength of a green HeNe laser. The emitted red light passed a dichroic mirror at 560 nm, was filtered using a 570-nm long-pass filter, and detected by a photomultiplier tube of a Zeiss LSM 410 confocal microscope mounted on an Axiovert M 135 (Zeiss, Oberkochen, Germany). Examination of the immunoreactivity using confocal laser scanning microscopy

Table 1. *Antibodies and Dilutions Used for Immunohistochemistry*

Antibody	Dilution
Rabbit anti-mouse collagen I (Institut Pasteur, Lyon, France)	1:200
Rabbit anti-mouse collagen IV (Institut Pasteur)	1:200
Rabbit anti-mouse fibronectin (Telios Pharmaceuticals, San Diego, CA)	1:200
Rabbit anti-mouse laminin (Institut Pasteur)	1:200
Rat anti-mouse ICAM-1 (R&D Systems, Minneapolis, MN)	1:100
Rat anti-mouse LFA-1 (R&D Systems)	1:100
Rat anti-mouse VLA-4 (Southern Biotechnologies, Birmingham, AL)	1:50
Rat anti-mouse VLA-6 (Serotec, Oxford, UK)	1:50
Rat anti-mouse F4/80 (macrophages) (Serotec)	1:200
Rabbit anti-mouse MCP (Serotec)	1:100
Mouse anti-human α-neurofilament (monoclonal negative control) (Dako, Glostrup, Denmark)	1:350
Rabbit anti-human IgM (polyclonal negative control) (Dako)	1:400
Goat anti-rat IgG, peroxidase conjugated (Rockland)	1:200
Goat anti-rabbit IgG, FITC conjugated Jackson Immunoresearch	1:25

yielded superior quality of the images compared with examination by conventional light microscopy. The degree of immunoreactivity was analyzed in a semi-quantitative manner (−, no reactivity; +, weak reactivity; ++, moderate reactivity; +++, strong reactivity).

Statistics

For all of the experimental groups (which included six to eight animals), the average volume and the standard deviation were calculated. The variables were compared by an unpaired, two-tailed Student *t*-test. Exact *P* values are given unless the *P* value was <0.0001.

Results

Mice with Unisexual Infections or with P. berghei Immunization

To obtain single-sex-infected snails, 50 *B. glabrata* snails were infected with a single miracidium each. Of the 50 infected snails, 5 yielded cercariae after 35 days. Analysis of perfused mice revealed that four snails had given rise to cercariae that developed into stunted male worms and one snail produced cercariae that developed into slender, thin female worms. Unisexually infected mice carried an average of 27.5 worms per animal (range, 20 to 39). The spleens from *P. berghei*-immunized mice (n = 9) and of a nonimmunized control group (n = 7) were weighed 8 days after injection. The spleens of the immunized animals weighed 0.93 ± 0.39 g *versus* 0.28 ± 0.23 g for the control animals ($P = 0.001$). With immunofluorescent antibody technique directed against sporozoite antigens, all serum samples had a strong fluorescent signal (+++) at a dilution of 1/80. The fluorescent signal was absent in serum samples of nonimmunized control mice.

Stereological Analysis

The results of the temporal stereological analysis of the MGV for both total (crude) SEA and a ConA binding fraction of SEA in naive and single-sex infected animals are represented in Table 2. The temporal MGV results for total SEA-induced granulomas are represented graphically in Figure 1. Quantification through stereological analysis revealed that, in unisexually infected animals, peak granuloma formation was already reached after 8 days (MGV = 5.45 ± 0.88 × 10^6 μm^3) whereas in naive animals peak granuloma formation was reached 16 days after injection (MGV = 6.33 ± 1.43 × 10^6 μm^3). In unisexually infected mice, strong granuloma formation was already observed after 3 days (MGV = 3.57 ± 0.71 × 10^6 μm^3), and the MGV at 8 days was significantly higher compared with naive mice at 8 days ($P < 0.0001$).

Table 2. *MGV (10^6 μm^3) of Total SEA- and ConA-Binding-Fraction-Induced Granulomas*

	Naive mice		Single-sex-infected mice	
Days	SEA	ConA binding	SEA	ConA binding
3			3.57 ± 0.71	2.30 ± 0.21
8	2.98 ± 0.36	2.75 ± 0.44	5.45 ± 0.88	3.58 ± 0.52
16	6.33 ± 1.44	4.48 ± 0.59	4.81 ± 0.75	3.14 ± 0.30
32	3.90 ± 0.65			

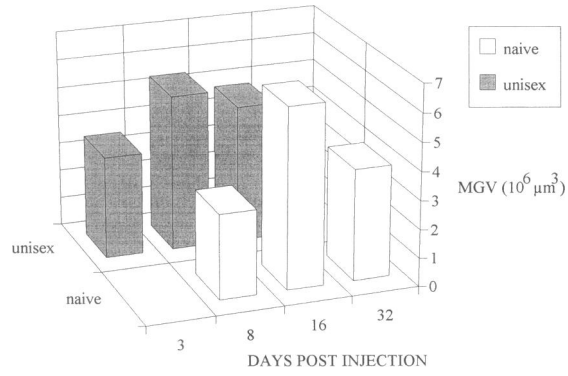

Figure 1. *Mean granuloma volume (MGV) of hepatic granulomas induced by SEA-coupled beads in naive and single-sex infected mice.*

At all stages both in naive and in unisexually infected mice, the ConA-binding-fraction-induced granulomas were smaller than total SEA-induced granulomas, reaching only 65 to 70% of the volume compared with SEA-induced granulomas.

No difference was observed in the MGV between unisexually and bisexually infected mice 8 days after injection (MGV, respectively, was 5.45 ± 0.88 and 5.50 ± 0.60 × 10^6 μm^3).

To assess worm specificity of the observed effect, SEA-induced granuloma formation was assessed in mice infected with *P. berghei* as compared with naive mice at 8 days after injection. Because the malarious animals were maintained at another institute, these animals were compared with a new group of naive (control) animals to ensure optimal environmental standardization of the experimental animals. *P. berghei*-immunized animals had a MGV of 2.98 ± 0.34 × 10^6 μm^3 compared with 2.85 ± 0.51 × 10^6 μm^3 for the naive animals ($P = 0.608$).

Conventional Light Microscopy

In all experimental groups, beads were found randomly lodged, although clustering of beads was sometimes observed, mainly in large portal veins. Seventy-two hours after injection of beads in single-sex-infected mice, the beads were surrounded by an initial layer of macrophages and several rows of lymphocytes, macrophages, and mainly eosinophilic granulocytes. Some neutrophilic granulocytes were seen. Small amounts of connective tissue were already observed. After 8 days, when peak granuloma formation was reached, large granulomas were seen (Figure 2a), composed of numerous eosinophils and macrophages. Sparse lymphocytes were seen, but neutrophils were absent. Giant cells were frequently seen at this stage, lying mainly against the bead. Marked fibrosis was present both in the granuloma and in areas of portitis. At 16 days, macrophages became the dominant cell type, but eosinophils were still abundantly present. Severe fibrosis was seen comprising the entire granuloma. Schistosomal pigment was present in Kupffer cells and phagocytic cells in the granuloma. A moderate to strong degree of portitis was observed with mainly eosinophils and macrophages. Some degree of piecemeal necrosis was seen. In naive animals, the same pattern of evolution was seen. However, at 8 days after injection, granulomas were still minute with small amounts of deposited collagen fibers. Full-blown granulomas with numerous eosinophils and marked fibrosis were seen after 16 days. At 32 days, fibrosis was marked with macrophages as the dominant cell type. Granulomas induced by ConA-binding-fraction-coupled beads had the same cellular composition as beads loaded with SEA. Unloaded beads yielded only a monolayer or bilayer of macrophages at all stages (Figure 2b). Malarious mice evoked granulomas in which eosinophils and macrophages were still the predominant cell types. Numerous Kupffer cells and granuloma macrophages were loaded with dark black malaria pigment.

Extracellular Matrix Protein Immunophenotyping

Collagen I immunoreactivity (Figure 2c) was seen as fine bands of granular deposits around the bead. Immunoreactivity for type I collagen was moderate in young granulomas in both naive and single-sex-infected mice but became more abundant as the granulomas aged. Immunoreactivity was also observed in the blood vessels and along the sinusoids. Collagen IV was absent along the sinusoids. Expression was seen in the basement membrane of the blood vessels. In the granuloma, periparticular bundles of type IV collagen (Figure 2d) were seen. Type IV collagen became more prominent when the granulomas grew older (16 and 32 days). Fibronectin (Figure 2e) lined the sinusoids and appeared to be the predominant ECM protein in the granulomas from the early stages on. Thick, dense bundles of fibronectin were seen in the granuloma. Laminin immunoreactivity was weakly expressed along the sinusoids. Strong reactivity was seen in the granuloma and in the blood vessels (Figure 2f). Significant deposition of ECM proteins was already observed 3 days after injection in single-sex-infected animals with peak deposition at 16 days. In naive animals, fibrosis was moderate at 8 days and became most pronounced at 32 days. Deposits of ECM proteins were not ob-

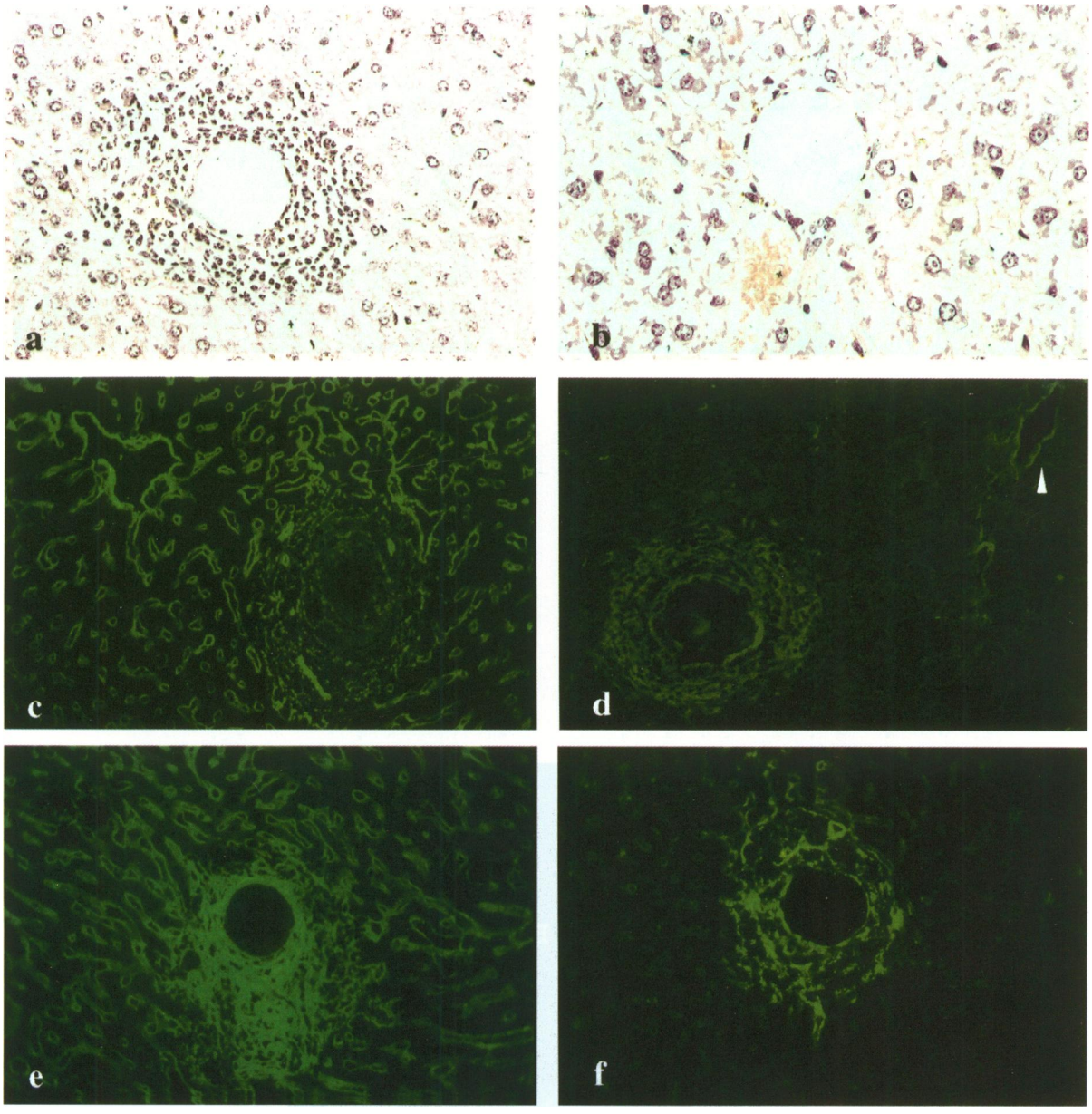

Figure 2. *Implantation of SEA-coupled or unloaded beads in the liver (8 days after injection) in unisexually infected mice.* a: *Granulomatous response against a SEA-coupled bead. Macrophages and numerous eosinophilic granulocytes make up the periparticular granuloma. H&E; magnification, ×180.* b: *Unloaded bead. No granulomatous response is seen except for a monolayer of schistosomal-pigment-laden macrophages. H&E; magnification, ×225.* c *to* f: *Deposition of type I collagen* (c), *type IV collagen* (d), *fibronectin* (e), *and laminin* (f) *around periparticular granulomas (8 days, single-sex infection). Fibronectin appeared the dominant ECM protein, whereas collagen I deposition was fine and granular. Type IV collagen was present in the granuloma and the basement membrane* (arrow) *of blood vessels. FITC; magnification, ×150.*

served around unloaded beads. Negative controls with an unrelated polyclonal antibody were negative in all cases. The results are summarized in Table 3.

Macrophages, Adhesion Molecules, and Chemokines

Granulomas were immunoreactive for the macrophage marker (F4/80) from the early stage on (3 days), and strong immunoreactivity persisted until

Table 3. *Extracellular Matrix Proteins in Single-Sex-Infected Animals 8 Days after Injection of SEA-Coated Sepharose Beads*

	Sinusoids	Granuloma	Blood vessels
Collagen type 1	+++	++	+++
Collagen type 4	–	++	++
Fibronectin	+++	+++	+++
Laminin	+	+++	+++

–, no reactivity; +, weak reactivity; ++, moderate reactivity; +++, strong reactiivity.

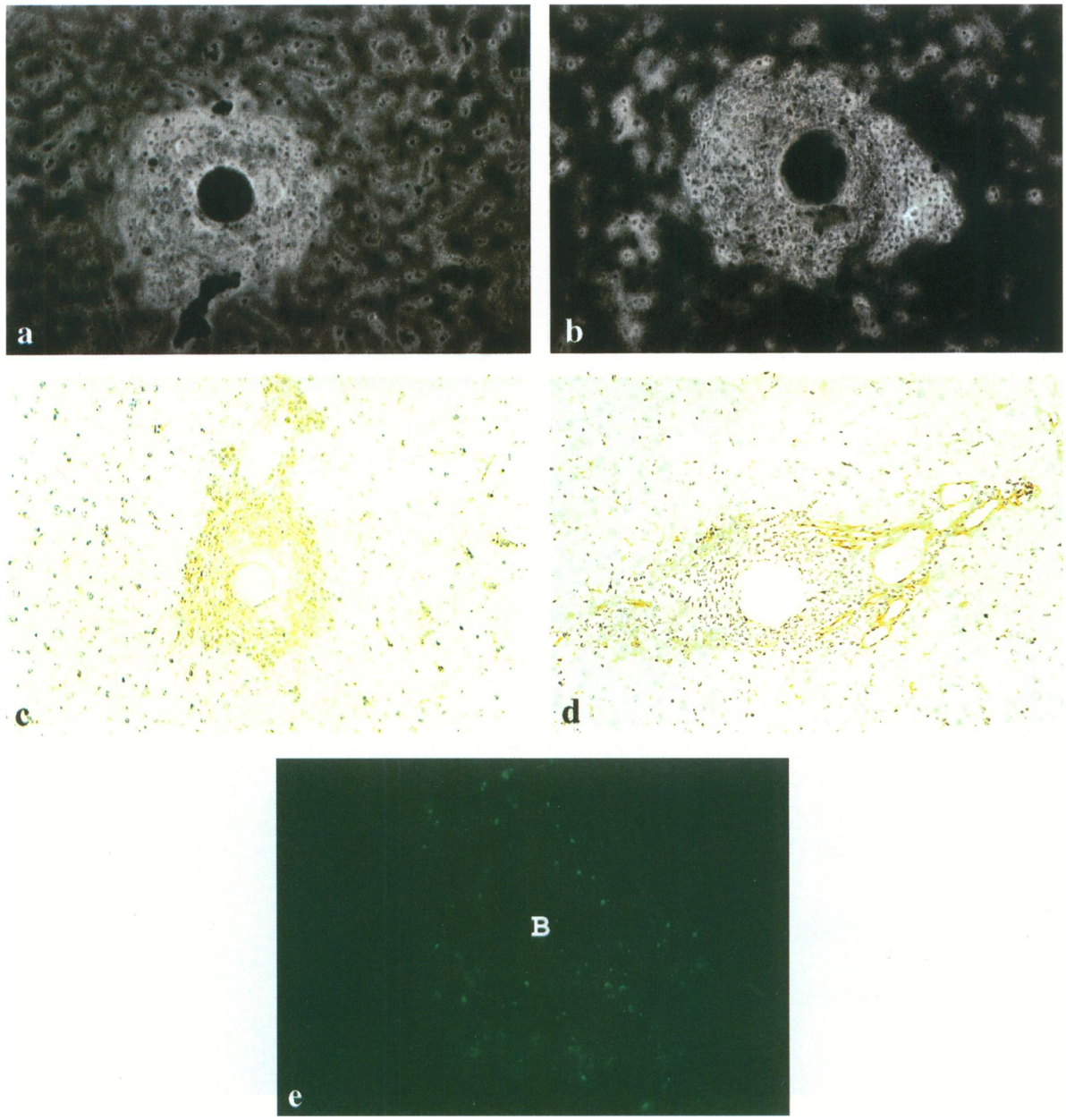

Figure 3. *Expression of adhesion molecules and chemokines on hepatic granulomas induced by injection of SEA-coupled beads (single-sex infected mice). Up-regulation of ICAM-1* (**a**), *LFA-1* (**b**), *and VLA-4* (**c**) *expression in periparticular granulomas is seen. VLA-6 expression in granulomas was less pronounced and limited to sparse, isolated granuloma cells and vascular endothelial cells encroached by the expanding granuloma.* **e**: *MCP-1-immunoreactive cells are present around implanted beads (B).* **a**: *confocal laser scanning microscope image; APAAP; magnification, ×120.* **b**: *CLSM image; APAAP; magnification, ×150.* **c** *and* **d**: *Indirect immunohistochemistry (peroxidase conjugate); hematoxylin counterstain; magnification, ×150.* **e**: *FITC; magnification, ×225.*

day 32. At day 3 after injection, most of the immunoreactivity was seen in cells in contact with the bead. At later stages, the granulomas stained homogeneously for the F4/80 monoclonal antibody. Clusters of F4/80-immunoreactive cells were seen in the inflamed portal tracts. Kupffer cells were immunoreactive, but the F4/80 immunoreactivity was absent in the vicinity of the central veins. ICAM-1 was present on sinusoidal lining cells (sinusoidal endothelium and schistosomal-pigment-phagocytizing Kupffer cells). ICAM-1 expression was strongly up-regulated on granuloma cells (Figure 3a). At the early stages (3 days), the granulomas stained homogeneously for ICAM-1. At the later stages (16 days), granulomas were observed with an unstained inner part. Areas of portitis were strongly ICAM-1 immunoreactive. Immunoreactivity for LFA-1 was seen in Kupffer cells with a pattern similar to the F4/80 macrophage

Table 4. *Macrophages, Adhesion Molecules, and Chemokines in Single-Sex-Infected Mice 8 Days after Injection of SEA-Coupled Sepharose Beads*

	Sinusoidal endothelium	Kupffer cells	Portal tract inflammatory cells	Hepatocytes	Granuloma inflammatory cells	Blood vessels
ICAM-1	+++	+++	+++	−	+++	+++, endothelium
LFA-1	−	+++	+++	−	+++	−
VLA-4	−	+	+++	−	++	−
VLA-6	++	−	+	−	+	+++, endothelium
MCP-1	−	−	−	−	++	++, adventitial cells in arteria hepatica branch
F4/80	−	+++	++	−	+++	−

−, no reactivity; +, weak reactivity; ++, moderate reactivity; +++, strong reactivity.

marker (Figure 3b) with decreased immunoreactivity toward the central vein. As for ICAM-1, granulomas stained homogeneously in the early stages, whereas in the later stages, the immunoreactivity pattern again became nonhomogeneous. Inflammatory cells in inflamed portal tracts were strongly immunoreactive. Immunohistochemical staining for VLA-4 (fibronectin receptor) revealed strong immunoreactivity on granuloma cells and portal tract inflammatory cells and weak immunoreactivity on schistosomal-pigment-laden Kupffer cells (Figure 3c). In areas of portitis, immunoreactivity was more pronounced near the lumen of the blood vessel and diminished at a distance. Endothelial cells were not immunoreactive. VLA-6 was predominantly expressed on the endothelial cells lining the central veins, the portal tract vessels, and blood vessels trapped in the granuloma, whereas moderate VLA-6 immunoreactivity was detected on sinusoidal endothelium (Figure 3d). Significant up-regulation of VLA-6 in the granuloma was not observed. Sparse immunoreactive cells were seen in the granulomas, mainly at the periphery, and in inflamed portal tracts. The bile duct epithelium was strongly immunoreactive. No expression was seen on hepatocytes and Kupffer cells. Sham-operated animals had weak basal expression of VLA-4 on Kupffer cells and moderate VLA-6 expression on endothelial cells. Moderate immunoreactivity for MCP-1 was seen in the granulomas of both unisexually infected and naive mice. Immunoreactivity was more pronounced in cells laying close to the antigen-coupled beads. As granulomas became larger in time, more MCP-1-immunoreactive cells were observed (Figure 3e). Vascular-associated MCP-1 was detected in the adventitial cells of hepatic artery branches in the portal tracts of single-sex-infected animals. Venous blood vessels were not immunoreactive. Few immunoreactive cells were seen in areas of portitis. In naive animals, vascular-associated immunoreactive cells were only sporadically seen. Blood vessels of sham-operated animals were not MCP-1 immunoreactive. No immunoreactivity was seen in the negative controls that were carried out for all antibodies. The weak immunoreactivity observed on some cell types for VLA-4 and VLA-6 could therefore not be attributed to detection of endogenous peroxidase by the indirect immunoperoxidase technique. The results are summarized in Table 4.

Discussion

In this communication, the results are shown of experiments aimed at identifying the role of adult, living *S. mansoni* worms on the hepatic granuloma formation *in vivo*. Sepharose beads laden with total SEA or a ConA binding fraction of SEA were injected in a mesenteric vein of naive, unisexually or bisexually (*S. mansoni*) infected and *P. berghei*-immunized mice, and the periparticular granuloma formation was analyzed by volume estimation through stereological analysis using point-sampled intercepts. In addition, the expression of adhesion molecules, chemokines, and ECM proteins was also studied. In this model, we demonstrated that peak granuloma formation was already reached after 8 days in single-sex-infected mice compared with 16 days in naive mice. Strong granuloma formation and deposition of ECM proteins was already seen 3 days after injection in single-sex-infected mice, whereas in naive animals, granuloma formation and fibrosis was still moderate 8 days after injection. This effect was not due to the aspecific arousal of the immune system, as triggering of the immune system with the nonrelated parasite *P. berghei* was not able to alter the SEA-induced granuloma formation. As one snail yielded cercariae that developed into female worms, the effect of worm gender on granuloma formation could be analyzed. In our experiments, mice carry-

ing female worms were present in only one experimental group (ConA binding fraction, 3 days after injection). When the MGV from this total group (male plus female worms; n = 7) was compared with the MGV of the female worm portion of the same group (n = 4), the respective MGVs were not significantly different (2.30 ± 0.21 and $2.40 \pm 0.2 \times 10^6$ μm^3; $P = 0.419$). As the experimental group carrying only female worms was small (only four mice), drawing definite conclusions from these data is hazardous. However, as no difference in MGV was observed between bisexually infected (28 days at the time of injection) and unisexually (male) infected (35 days) mice, the positive immunomodulation by *S. mansoni* worms on SEA-induced granulomas is most likely independent of the worm gender or degree of female worm maturation. In addition Grzych et al[13] did not observe differences between SWAP prepared from male, female, and unseparated worms in its capacity to trigger spleen cell cytokine responses.

Preliminary results of experiments performed in our laboratory demonstrate that Sepharose beads coupled with total adult worm antigen (AWA), hence containing worm antigens not only from male and female worms but also antigens from eggs present in the uterus of female worms, induced granulomas with the same size as that of granulomas induced by SEA-coupled beads in unisexually or bisexually infected animals. When beads coated with exclusively adult, male worm antigens (and thus free of egg antigens) were injected, these also generated granulomas but of a smaller size (W. Jacobs, J. Bogers, A. Deelder, and E. Van Marck, unpublished results). The formation of large granulomas by total-AWA-coupled beads is likely to be partly attributable to cross-reaction of AWA with SEA. In addition, these preliminary results demonstrate that AWA has granulomogenic potential *in vivo*. Hirsch and Goes[16] very recently described that adult worm antigen fractions coupled to polyacrylamide beads were able to induce a granulomatous reaction *in vitro*. Doughty and Phillips[31] observed that *in vitro* granuloma formation around *S. mansoni* eggs was strongly accelerated when *S. mansoni* worms and eggs were co-cultured with spleen cells. This acceleration was not observed when only eggs and spleen cells were co-cultured. From these results obtained *in vitro*, these authors were not able to conclude whether the observed phenomenon indicated the presence of sensitizing cross-reactive worm antigens or the necessity for conditioned media to facilitate the cellular reactions. Our present *in vivo* work supports the hypothesis that the positive immune modulation by *S. mansoni* worms is mediated possibly by two mechanisms: the presence of granulomogenic worm antigens and sensitizing cross-reaction between egg and worm antigens. Interaction and cross-sensitization between egg and worm antigens has previously been described. Lukacs and Boros[10] defined from nine SEA fractions five fractions that induced pulmonary granulomas in acutely infected (8 weeks) mice. Only four fractions were granulomogenic in chronically infected (20 weeks) mice. Some of these fractions were cross-reactive with schistosomular antigens at the T-cell level.[11] The granulomatous response appeared to be a composite T-cell reactivity to several larval cross-reactive and egg-specific antigenic moieties.

It has been shown[26,32] that the ConA binding fraction contains major serological antigen-1 (MSA-1) and that this antigen is responsible for a granulomatous reaction with subsequent fibrosis when attached to particles and implanted in the liver of mice.[15] Because ConA-binding-fraction-induced granulomas were smaller in both naive and single-sex-infected mice, it is reasonable to assume that SEA contains, besides MSA-1, other granulomogenic antigens that act in synergy with MSA-1 for eliciting schistosomal delayed hypersensitivity.

Conflicting results exist between the pulmonary and hepatic granuloma formation in single-sex-infected mice. Warren and Domingo[33] did not observe a difference in the pulmonary granulomatous response against *S. mansoni* eggs in naive and single-sex-infected mice. In apparent disagreement with that result, in our current and earlier studies,[15] unisexually infected mice exhibited an augmented hepatic granulomatous response to SEA-coupled beads. It was, however, demonstrated that hepatic granulomas of mice infected with *S. mansoni* sequester immunogenic epitopes expressed by the worm.[34] As the liver is a major organ for the clearance of many macromolecules from the circulation,[35] it may sequester schistosome antigens from developmental stages other than eggs.[36] Circulating anodic antigen has been detected in Kupffer cells,[37,38] and hepatic clearance of schistosomal worm antigens could be due to binding of the antigens to specific carbohydrate receptors on hepatocytes and Kupffer cells.[39] Artificial bead- or egg-induced pulmonary granulomas may thus be a good model for the elucidation of the immunological mechanisms underlying schistosomiasis,[10,22,40,41] but artificial hepatic granulomas provide a more realistic model for unraveling the pathology of schistosomiasis.[9] It has been demonstrated that differences between hepatic and pulmonary granulomas exist, particularly at the morphological level.[42] Hepatic granulomas

are larger and give rise to more fibrosis than pulmonary granulomas do,[43] whereas vasculitis is a common feature in the lung.[42] The differences in organ-related reaction patterns toward antigenic stimuli and the sequestration capacity of the liver for schistosome antigens may explain the lack of immunomodulation by adult worms on pulmonary granulomas observed by Warren and Domingo.[33]

Synchronous hepatic granulomas have proven to be a good model for the study of hepatic fibrosis.[15,44] In our experiments, we noticed deposition of collagen isotypes and basement membrane molecules in the artificial granulomas. In experimental murine infections, type III collagen and fibronectin are the dominant ECM proteins in the initial hepatic lesions (8 weeks after infection) whereas an increase of type IV collagen and laminin deposition was seen at 10 weeks after infection. As the infection progressed, type I collagen deposits rose and equalled type III collagen.[45] We did not evaluate type III collagen expression in our model because an antibody directed against mouse collagen type III was not commercially available at that time. Andrade[46] reported that type IV collagen was not involved in schistosomal fibrosis, but Kresina et al[47] nevertheless observed type IV collagen gene expression during primary infection. We previously observed that ICAM-1 immunoreactivity at the ultrastructural level was present on both Kupffer cells and sinusoidal endothelium.[48] We also observed a reduction of ICAM-1 and LFA-1 staining in advanced infections (22 weeks) or in granulomas around SEA beads deposited for a longer period (32 days),[48] with ICAM-1-immunoreactive cells mainly located at the periphery of the granuloma in contrast to the homogeneous staining of the granuloma during the acute phase. This reduction of ICAM-1 staining persisted after collagenase pretreatment, suggesting that this phenomenon was due to the presence of nonimmunoreactive cells rather than to masking of the antigen by connective tissue fibers. Ritter and McKerrow[49] very recently described the same phenomenon in experimental infections and demonstrated that ICAM-1 was the major adhesion molecule expressed during schistosome granuloma formation. The up-regulation of ICAM-1, LFA-1, and VLA-4 expression on cells of the periparticular granuloma, strongly during the acute and to a lesser degree during the late phase of granuloma formation, gives additional evidence for the role of adhesion molecules in the initiation and maintenance of granulomogenesis. The chemokine MCP-1 was both granuloma and vascular associated during secondary pulmonary granuloma formation.[22] MCP-1 immunoreactivity in the adventitial cells of arterioles and in the lung granulomas during secondary (infected mice) pulmonary granuloma formation was noticed. The authors did not observe vascular immunoreactivity during primary (naive mice) pulmonary granuloma formation. Our observations confirm these findings in the liver. Granuloma immunoreactivity for MCP-1 was seen in both naive and single-sex-infected mice, but arterial immunoreactivity was present only in single-sex-infected mice. Maybe the presence of circulating worm antigens constitutes a stimulus for inflammatory cells to secrete larger amounts of chemokines with pro-inflammatory action, increasing granuloma cellularity. From this study, it is concluded that the presence of living adult *S. mansoni* worms has an important positive immunomodulatory effect on hepatic granuloma formation *in vivo*. This effect is likely to be attributable to cross-reactivity of AWA with SEAs although the influence of granulomogenic adult worm antigens has to be taken into consideration. Artificial hepatic granulomas in single-sex-infected animals provide a good model for the study of hepatic fibrosis. Adhesion molecules and chemokines constitute important inflammatory components in artificial hepatic granulomas.

Acknowledgments

We thank D. Kornelis, L. Moeneclay, L. Dierickx, F. Lockefeer, and F. Rylant for the excellent technical assistance. The surgical assistance of Dr. J. Hendriks was kindly appreciated.

References

1. Biguet J, Capron A, Tran Van Ky P: Les antigènes de *Schistosoma mansoni*. I. Etude électrophorétique: charactérisation des antigènes specifiques. Ann Inst Pasteur 1962, 103:763–777
2. Capron A, Biguet J, Vernes A, Afchain D: Structure antigénique des helmintes: aspects immunologiques des relations hôte-parasite. Pathol Biol 1968, 16:121–138
3. Boros DL: Immunopathology of *Schistosoma mansoni* infection. Clin Microbiol Rev 1989, 2:250–269
4. Boros DL, Pelley RP, Warren KS: Spontaneous modulation of granulomatous hypersensitivity in schistosomiasis mansoni. J Immunol 1975, 114:1437–1441
5. Boros DL, Warren KS: Delayed hypersensitivity granuloma formation and dermal reaction induced and elicited by a soluble factor isolated from *Schistosoma mansoni* eggs. J Exp Med 1970, 132:488–507
6. Boros DL, Tomford R, Warren KS: Induction of granulomatous and elicitation of cutaneous sensitivity by par-

tially purified SEA of *Schistosoma mansoni*. J Immunol 1977, 118:373–376
7. Harrison DJ, Carter CE, Colley DG: Immunoaffinity purification of *Schistosoma mansoni* soluble egg antigens. J Immunol 1979, 122:2210–2216
8. Lustigman S, Mahmoud AAF, Hamburger J: Glycoproteins in soluble egg antigen of *Schistosoma mansoni*: isolation, characterization, and elucidation of their immunochemical and immunopathological relation to the major egg glycoprotein (MEG). J Immunol 1985, 134: 1961–1967
9. Weis JB, Aronstein WS, Strand M: *Schistosoma mansoni*: stimulation of artificial granuloma formation *in vivo* by carbohydrate determinants. Exp Parasitol 1987, 64:228–236
10. Lukacs NW, Boros DL: Utilization of fractionated soluble egg antigens reveals selectively modulated granulomatous and lymphokine responses during murine schistosomiasis. Infect Immun 1992, 60:3209–3216
11. Lukacs NW, Boros DL: Identification of larval cross-reactive and egg-specific antigens involved in circumoval granuloma formation in murine schistosomiasis mansoni. Infect Immun 1991, 59:941–948
12. Williams ME, Montenegro S, Domingues AL, Wynn TA, Teixeira K, Mahanty S, Coutinho A, Sher A: Leukocytes of patients with *Schistosoma mansoni* respond with a Th2 pattern of cytokine production to mitogen or egg antigens but with a Th0 pattern to worm antigens. J Infect Dis 1994, 170:946–954
13. Grzych JM, Pearce E, Cheever A, Caulada ZA, Caspar P, Heiny S, Lewis F, Sher A: Egg deposition is the major stimulus for the production of Th2 cytokines in murine schistosomiasis mansoni. J Immunol 1991, 146:1322–1327
14. Araújo MI, Ribeiro de Jesus A, Bacellar O, Sabin E, Pearce E, Carvalho EM: Evidence of a T helper type 2 activation in human schistosomiasis. Eur J Immunol 1996, 26:1399–1403
15. Van Marck EAE, Kestens L, Stocker S, Grimaud JA, Gigase PLJ, Deelder AM: Fibrosis around schistosomal egg antigen-coated beads in the liver of mice. Contr Microbiol Immunol 1983, 7:251–259
16. Hirsch C, Goes AM: Characterization of fractionated *Schistosoma mansoni* soluble adult worm antigens that elicit human cell proliferation and granuloma formation *in vitro*. Parasitology 1996, 112:529–535
17. Ritter DM, Rosen S, McKerrow JH: Induction of ICAM-1 expression by products of the deposited egg of *Schistosoma mansoni*. Abstr Exp Biol 1994, Abstr 1342, p A232
18. Lukacs NW, Chensue SW, Strieter RM, Warmington K, Kunkel SL: Inflammatory granuloma formation is mediated by TNF-α-inducible intercellular adhesion molecule-1. J Immunol 1994, 152:5883–5889
19. Langley JG, Boros DL: T-lymphocyte responsiveness in murine schistosomiasis mansoni is dependent upon adhesion molecules intercellular adhesion molecule-1, lymphocyte function-associated antigen-1, and very late antigen-4. Infect Immun 1995, 63:3980–3986
20. Shimizu Y, van Seventer GA, Horgan KJ, Shaw S: Regulated expression and function of three VLA(β1) integrin receptors on T cells. Nature 1990, 345:250–253
21. Tanaka Y, Adams DH, Hubscher S, Hirano H, Siebenlist U, Shaw S: T-cell adhesion induced by proteoglycan-immobilized cytokine MIP-1β. Nature 1993, 361: 79–82
22. Chensue SW, Warmington KS, Lukacs NW, Lincoln PM, Burdick MD, Strieter RM, Kunkel SL: Monocyte chemotactic protein expression during schistosome egg granuloma formation. Am J Pathol 1995, 146:130–138
23. Lukacs NW, Kunkel SL, Strieter RM, Warmington K, Chensue SW: The role of macrophage inflammatory protein 1α in *Schistosoma mansoni* egg-induced granulomatous inflammation. J Exp Med 1993, 177:1551–1559
24. Deelder AM, Snoijink JJ, Ploem JS: Experimental optimization of the DASS system for immunodiagnosis of some helminth infections. Ann NY Acad Sci 1975, 254: 119–134
25. Browne HG, Thomas JI: A method for isolating pure, viable schistosome eggs from host tissues. J Parasitol 1953, 49:371–374
26. Pelley RP, Pelley RJ, Hamburger J, Peters PA, Warren KS: *Schistosoma mansoni*: soluble antigens. I. Identification and purification of three major antigens, and the employment of radioimmunoassay for their further characterization. J Immunol 1976, 117:1553–1560
27. Laughlin LW: Schistosomiasis. Hunter's Tropical Medicine, ed 6. Edited by GT Strickland. Philadelphia, WB Saunders Co, 1984, pp 708–740
28. Baak JPA, Oort J, Fleege JC, Van Diest PJ, Ploem JS: Techniques in quantitative pathology. Manual of Quantitative Pathology in Cancer Diagnosis and Prognosis. Edited by JPA Baak. Heidelberg, Springer Verlag, 1991, pp 45–56
29. Gundersen HJG, Jensen EB: Particle sizes and their distributions estimated from line- and point-sampled intercepts, including graphical unfolding. J Microsc 1983, 131:291–310
30. Murdoch A, Jenkinson EJ, Johnson GD, Owen JJ: Alkaline phosphatase-fast red, a new fluorescent label: application in double labelling for cell surface antigen and cell cycle analysis. J Immunol Methods 1991, 139: 149–151
31. Doughty BL, Phillips MS: Delayed hypersensitivity granuloma formation around *Schistosoma mansoni* eggs *in vitro*. I. Definition of the model. J Immunol 1982, 128:30–36
32. Hamburger J, Pelley RP, Warren KS: *Schistosoma mansoni* soluble egg antigens: determination of the stage and species specificity of their serological reactivity by radioimmunoassay. J Immunol 1976, 117:1561–1566
33. Warren KS, Domingo EO: *Schistosoma mansoni*: stage specificity of granuloma formation around eggs after

exposure to irradiated cercariae, unisexual infections or dead worms. Exp Parasitol 1970, 27:60–66
34. Salama MMA, Aronstein WS, Weiss JB, Strand M: Monoclonal antibody identification of protein antigens in the liver of mice infected with *Schistosoma mansoni*. Am J Trop Med Hyg 1984, 33:608–620
35. Bogers JJ, Nibbeling HA, Deelder AM, Van Marck EA: Immunohistochemical and ultrastructural localization of *Schistosoma mansoni* soluble egg antigens processed by the infected host. Parasitology 1996, 112:537–543
36. Nash TE: Factors that modulate clearance and ultimate fate of a specific schistosome antigen (GASP) in schistosome infections. J Immunol 1982, 128:1608–1613
37. Van Marck E: Presence of the circulating polysaccharide antigen in the liver of mice infected with *Schistosoma mansoni*. Ann Soc Belg Med Trop 1975, 55:373–377
38. Deelder AM, Kornelis D, Van Marck EAE, Eveleigh PC, Van Emond JG: *Schistosoma mansoni*: characterization of two circulating polysaccharide antigens and the immunological response to these antigens in mouse, hamster, and human infection. Exp Parasitol 1980, 50: 16–32
39. Neufeld EF, Ashwell G: Carbohydrate recognition systems for receptor mediated pinocytosis. The Biochemistry of Glycoproteins and Proteoglycans. Edited by WJ Lennarz. New York, Plenum Publishing, 1980, pp 241–266
40. Lukacs NW, Boros DL: Lymphokine regulation of granuloma formation in murine schistosomiasis mansoni. Clin Immunol Immunopathol 1993, 68:57–63
41. Chensue SW, Warmington K, Ruth J, Lincoln P, Kuo MC, Kunkel SL: Cytokine responses during mycobacterial and schistosomal antigen-induced pulmonary granuloma formation. Am J Pathol 1994, 145:1105–1113
42. Edungbola LD, Schiller EL: Histopathology of hepatic and pulmonary granulomata experimentally induced with eggs of *Schistosoma mansoni*. J Parasitol 1979, 65:253–261
43. Eltoum IA, Wynn TA, Poindexter RW, Finkelman FD, Lewis FA, Sher A, Cheever AW: Suppressive effect of interleukin-4 neutralization differs for granulomas around *Schistosoma mansoni* eggs injected into mice compared with those around eggs laid in infected mice. Infect Immun 1995, 63:2532–2536
44. Stocker S, Van Marck EAE, Deelder AM, Kestens L, Gigase PLJ, Grimaud JA: Hepatic schistosomal fibrosis: ultrastructural study of experimentally induced periparticular reaction. Contr Microbiol Immunol 1983, 7:260–266
45. Grimaud JA, Boros DL, Takiya C, Mathew RC, Emonard H: Collagen isotypes, laminin and fibronectin in granulomas of the liver and intestines of *Schistosoma mansoni*-infected mice. Am J Trop Med Hyg 1987, 37:335–344
46. Andrade ZA, Grimaud JA: Evolution of the schistosomal hepatic lesions in mice after curative chemotherapy. Am J Pathol 1986, 124:59–65
47. Kresina TF, He Q, Degli Esposti S, Zern MA: Gene expression of transforming growth factor-β1 and extracellular matrix proteins in murine *Schistosoma mansoni* infection. Gastroenterology 1994, 107:773–780
48. Jacobs W, Bogers J, Deelder A, Van Marck E: ICAM-1 and LFA-1 expression in experimental *Schistosoma mansoni* infection and in synchronous periparticular hepatic granulomas in mice: immunohistochemistry, confocal laser scanning microscopy, and immunoelectron microscopy. Parasitol Res (in press)
49. Ritter DM, McKerrow JH: Intercellular adhesion molecule 1 is the major adhesion molecule expressed during schistosome granuloma formation. Infect Immun 1996, 64:4706–4713